

Loss of polymeric immunoglobulin receptor expression is associated with lung tumorigenesis

Sebahat Ocak^{1,7,8}, Tetyana V. Pedchenko¹, Heidi Chen², Fredrick T. Harris^{1,6}, Jun Qian¹,
Vasiliy Polosukhin¹, Charles Pilette^{9,10}, Yves Sibille^{7,8}, Adriana L. Gonzalez³, Pierre P.
Massion^{1,4,5}

¹Division of Allergy, Pulmonary and Critical Care Medicine, Vanderbilt University (VU), Nashville, Tennessee; ²Cancer Biostatistics Center, VU, Nashville, Tennessee; ³Department of Pathology, VU, Nashville, Tennessee; ⁴Vanderbilt-Ingram Comprehensive Cancer Center, Nashville, Tennessee; ⁵Division of Allergy, Pulmonary and Critical Care Medicine, Veterans Affairs, Tennessee Valley Health Care Systems, Nashville, Tennessee; ⁶Department of Biochemistry and Cancer Biology, Meharry Medical College, Nashville, Tennessee; ⁷Unit of Microbiology, Université Catholique de Louvain (UCL), Brussels, Belgium; ⁸Division of Pulmonary Medicine, Cliniques Universitaires Mont-Godinne, UCL, Yvoir, Belgium; ⁹Institute of Experimental and Clinical Research, Pole of Pneumology, ENT and Dermatology, UCL, Brussels, Belgium; ¹⁰Division of Pulmonary Medicine, Cliniques Universitaires St-Luc, UCL, Brussels, Belgium

Corresponding author:

Pierre P. Massion, M.D.

Division of Allergy, Pulmonary and Critical Care Medicine

Vanderbilt-Ingram Cancer Center

2220 Pierce Avenue, Preston Research Building 640

Nashville TN 37232-6838

Tel: 615-936-2256

Fax: 615-936-1790

E-mail: pierre.massion@vanderbilt.edu

Running title:

pIgR loss is associated with lung tumorigenesis

Title: 90 characters (with spaces)

Running title: 47 characters (with spaces)

Abstract: 200 words

Key words: 6

Manuscript (excluding abstract, acknowledgements, references, tables and figure legends): 3062 words

References: 32

Figures: 6

Tables: 2

Supplementary figure: 1

Supplementary tables: 2

Abstract

Rationale: Polymeric immunoglobulin receptor (pIgR) expression is downregulated in lung cancer, but implications in lung tumorigenesis remain unknown. We hypothesized that loss of pIgR expression occurs early, is associated with cell proliferation and poor prognosis.

Methods: pIgR expression was evaluated by immunohistochemistry in airways of patients with normal mucosa, preinvasive and invasive lesions and correlated with clinical outcomes. 16-HBE and A549 cells stably transfected with pIgR were tested for proliferation, apoptosis and cell cycle.

Results: Immunostaining was strong in normal epithelium, but severely reduced in preinvasive lesions and most lung cancers. Persistent expression was associated with younger age and adenocarcinoma subtype but not survival. pIgR overexpression significantly reduced A549 and 16-HBE proliferation. Growth inhibition was not due to cell cycle arrest, increased apoptosis or endoplasmic reticulum stress but we observed altered expression of genes encoding for membrane proteins, including NOTCH3. Interestingly, NOTCH3 expression was inversely correlated with pIgR expression in cell lines and tissues.

Conclusion: pIgR expression was lost in most lung cancers and preinvasive bronchial lesions, suggesting that pIgR downregulation is an early event in lung tumorigenesis. pIgR overexpression in A549 and 16-HBE inhibited proliferation. Future investigations are required to determine mechanisms by which pIgR contributes to cell proliferation.

Key words

Differentiation, lung adenocarcinoma, lung preinvasive lesions, pIgR, proliferation.

Introduction

Transmembrane receptors are critical in cellular signaling and regulate proliferation, host defense mechanisms and cellular homeostasis. Polymeric immunoglobulin receptor (pIgR) is a transmembrane glycoprotein expressed in mucosal surfaces that mediates polymeric IgA (pIgA) transcytosis from the basolateral pole to the apical surface of epithelial cells [1, 2]. At cell's luminal surface, pIgR is cleaved and its extracellular ligand-binding region, called secretory component (SC), is released free or binding pIgA in a complex called secretory IgA (SIgA). SIgA is the first line of immunological defence against environmental antigens mucosal surfaces are exposed to [3, 4].

Under normal condition, pIgR is highly expressed in epithelial cells of the upper respiratory tract (mainly serous, also mucous and ciliated cells), while the expression is absent in alveolar cells [5]. pIgR expression has been reported to be downregulated in various lung diseases, including COPD [5], fibrosis [6], sarcoidosis [6] and cancer [7-13]. Several studies have shown that pIgR expression is decreased in lung adenocarcinomas (ADCs), with lower expression in poorly differentiated tumors, and absent in other lung cancer types [7-13]. Decreased pIgR expression has also been described in other cancers [14-18]. In colo-rectum, pIgR downregulation was observed in cancerous and preinvasive lesions, with lower expression in poorly differentiated lesions [16, 18]. Moreover, pIgR expression in colorectal cancer was associated with outcome and proposed as a prognostic biomarker [14, 16-18].

Mechanisms leading to pIgR downregulation in lung cancer are poorly understood. pIgR mRNA levels have been correlated with the expression of constitutional transcription factors USF1/2 and AP2- α [19].

The temporality of pIgR downregulation in lung tumorigenesis is unknown and we don't know whether pIgR downregulation carries prognostic value. Moreover, biological

implications of pIgR downregulation in lung cancer development/progression have not been reported. We therefore formulated the following three hypotheses: pIgR downregulation is an early event in lung tumorigenesis, is associated with poor prognosis and has biological implications in lung cancer development. To test these hypotheses, we determined pIgR expression by immunohistochemistry (IHC) in lung preinvasive and invasive tumors, correlated pIgR staining to clinical outcomes and evaluated the effects of pIgR overexpression on proliferation, cell cycle progression and apoptosis. Addressing these hypotheses may improve our understanding of the molecular steps leading to lung cancer and the role of a critical cellular receptor involved in cell trafficking and differentiation regulation.

Material and methods

Tissues, cell lines

Non-small cell lung cancer (NSCLC) samples from 175 patients without prior medical treatment were assembled in tissue microarrays (TMAs) prepared from paraffin blocks obtained from the archives of the Pathology Department at Vanderbilt University Medical Center and Nashville VA Medical Center, Tennessee. Lung cancer diagnosis was confirmed by a lung cancer pathologist (ALG) and samples were annotated with clinical data elements. The study was approved by Institutional Review Boards. Snap-frozen tissues from 11 patients with lung ADC and six with SCC were obtained through Vanderbilt Specialized Program of Research Excellence in lung. The following cell lines were purchased from ATCC (Manassas, VA): BEAS-2B, NCI-H1299, NCI-H460, NCI-H226, NCI-H520, NCI-A549, Calu-3, NCI-H23, NCIH2009, NCI-H1650, NCI-H1819 and NCI-H1993. 16-HBE was a kind gift from Dr. Gruenert (Children's Hospital, Oakland Research Institute). H157, HCC15, HCC95, H549, HCC78 were kind gifts from Dr. Minna (University of Texas Southwestern). All cells were cultured under recommended conditions.

Immunohistochemistry

TMAs were stained following previously reported protocol [5]. Briefly, slides were incubated overnight at 4°C with anti-human pIgR/SC polyclonal goat IgG (1:500; goat 606 prepared in Dr. Sibille's laboratory). The secondary antibody, biotinylated rabbit anti-goat IgG from the VECTASTAIN Elite ABC system (1:50; Vector Laboratories, Burlingame, CA), was applied at room temperature for 30 min. Staining intensity was evaluated by two independent observers (ALG, SO): 0-no, 1-weak, 2-moderate, and 3-strong staining. Staining intensity was multiplied by stained tumor cells percentage to obtain the final staining score (range=0-300), used for association with clinical outcomes.

Western blotting

Lysates were obtained from cells/tissues following standard protocol [20]. Blots were probed with antibodies against human pIgR/SC (1µg/ml; polyclonal rabbit IgG (rabbit 877) prepared in Dr. Sibille's laboratory), calreticulin (1:1000; Cell Signaling, Danvers, MA), BIP (1:1000; Santa Cruz Biotechnology, Santa Cruz, CA), NOTCH3 (1:1000; Orbigen, San Diego, CA) or actin (1:5000; Sigma, St. Louis, MO).

Stable transfection with pIgR- or empty vector-pcDNA3.1(-)

A549 or 16-HBE cells were seeded in six-cm dishes at 2×10^5 and 12×10^5 cells/dish respectively. Next day, transfection of human pIgR cDNA (kind gift from Dr. Kaetzel, University of Kentucky) [21] in pcDNA3.1(-) (Invitrogen, Carlsbad, CA) or empty pcDNA3.1(-) was performed using PolyFect Transfection Reagent (Qiagen, Valencia, CA) according to manufacturer's instructions. Two days later, cells were split and medium was supplemented with geneticin (600µg/ml for A549, 100µg/ml for 16-HBE; Gibco, Carlsbad, CA). After two weeks, geneticin-resistant clones were picked and tested for pIgR expression.

Proliferation assay

Stably transfected A549 and 16-HBE cells were seeded in 96-well plates at 0.5×10^3 cells/well and 5×10^3 cells/well respectively. They were cultured in 10%-FBS medium for six days. Every day, WST-1 reagent (Roche, Mannheim, Germany) was used for spectrophotometric quantification of cell proliferation per manufacturer's instructions.

Apoptosis assay

Stably transfected A549 cells were seeded in six-cm dishes at 2×10^5 cells/dish. Two days later, cells were stained with 100µl AnnexinV binding buffer containing 1µl Alexa Fluor®-

488-conjugated AnnexinV (Invitrogen, Carlsbad, CA) and 1µl Propidium Iodide (PI) (100µg/ml; Sigma, St. Louis, MO). Staining was quantified by FACS analysis. Data acquisition and analysis were performed with CellQuestpro (BD Biosciences, San Jose, CA).

Cell cycle analysis

Stably transfected A549 cells were seeded in six-cm dishes at 2×10^5 cells/dish. Next day, 10%-FBS medium was replaced by serum-free medium (synchronization). Cells were pelleted and fixed with ethanol at different timepoints (0-4-8-12-20-22-24-26h). Cells were with 1ml PI (100µg/ml; Sigma, St. Louis, MO) and RNaseA (100 µg/ml; Qiagen, Valencia, CA). A total of 10,000 stained nuclei were subjected to flow cytometry. Data were collected on a Becton Dickinson FACSCalibur flow cytometer using CellQuest Pro (BD Biosciences, San Jose, CA). Cell cycle analysis was done with ModFit LT software (Verity Software House, Topsham, ME).

Gene expression microarray analysis

Total RNA was isolated from stably transfected A549 after three days of culture using TRIzol (Invitrogen, Carlsbad, CA), following manufacturer's protocol. RNA was hybridized to a GeneChip[®] Human Genome U133 Plus 2.0 Array (Affymetrix, Santa Clara, CA). Image analysis was performed by Vanderbilt University DNA Microarray Core Facility. Data were analyzed with Expression Console (Affymetrix, Santa Clara, CA). Experiments were performed three times.

Statistical analyses

Immunohistochemistry. Wilcoxon rank-sum or Kruskal-Wallis tests were used to correlate pIgR average staining scores with categorical clinico-pathological outcomes and Spearman's

rank test was used for continuous outcomes. Overall survival was calculated from date of diagnosis to date of death or last date of contact for those alive at the time of analysis. Recurrence/progression-free survival was calculated from date of diagnosis to date of recurrence/progression or last date of contact for those without recurrence/progression at the time of analysis. Score test was used for survival analyses. Kaplan-Meier survival curves were calculated according to pIgR expression (staining score =0 versus >0 and <20 versus ≥ 20) and compared using log-rank test. Descriptive statistics, including median and inter-quartile ranges for continuous and percentages or frequencies for categorical variables, were reported. Multivariable analyses were performed using Cox proportional-hazards model to adjust for age, pack years, lung cancer histology and stage. All tests were two-sided, and p-values <0.05 were considered statistically significant. Analyses were performed using R 2.9.2.

Gene expression microarray. Data were normalized by using the Robust Multi-chip Average. Candidate genes were selected based on two-fold change of gene expression in A549 overexpressing pIgR, and p values of Student's t-test <0.05.

Results

pIgR expression is downregulated early in lung tumorigenesis

pIgR expression was evaluated by IHC in the airways during bronchial tumor development. Results are summarized in Table 1, and representative images are shown in Figures 1A-1F. pIgR expression was cytosolic and membranous, in accordance with its role as transcytosed membrane receptor. pIgR was expressed in 10/11 normal bronchial and alveolar tissues, with strong intensity in mucous and serous cells of surface and glandular epithelium, weak intensity in ciliated and an expected absence of staining in alveolar cells. In all tested lung preinvasive lesions (four low- and six high-grade), we observed an absence of pIgR expression, suggesting that pIgR downregulation is an early event during lung tumorigenesis. Staining of lung cancer TMAs including samples from 175 patients demonstrated an absence of pIgR expression in all undifferentiated NSCLCs, 60/67 SCCs and 47/98 ADCs.

pIgR expression was then evaluated by WB in lung cancer and normal lung tissues from same patients (Figure 2A). pIgR expression was downregulated in 6/6 SCCs. In ADCs, downregulation was observed in 5/11, while there was no expression difference in 2/11 and even overexpression in 4/11 tissues. These results were consistent with those observed by IHC. In cell lines, pIgR expression was low in 2/2 immortalized normal bronchio-epithelial, 1/1 NSCLC, 1/1 LCC, 5/5 SCCs and 7/9 ADCs. Expression was moderate in HCC78 and strong in Calu-3, both being of ADC subtype (Figure 2B).

pIgR expression is associated with age and histology

pIgR staining scores were correlated with clinical and pathological variables. Patient characteristics and the statistical significance of the correlations between pIgR staining and

these clinico-pathological variables are summarized in Table 2. Staining scores treated as continuous variables were significantly higher in younger patients ($p=0.041$) and those with ADC ($p<0.0001$). Staining scores were also treated as categorical variables ($=0$ versus >0 and <20 versus ≥ 20), and this revealed similar results (data not shown). Staining scores were not significantly associated with other variables, especially disease stage, overall (Figure 1G) and recurrence/progression-free survivals (Figure 1H). These observations were also true in the ADC subgroup.

pIgR overexpression inhibits lung cancer cell proliferation

Although pIgR is downregulated in lung cancer, its implication in tumorigenesis remains unknown. Therefore we tested whether pIgR contributes to cellular functions important for cancer development/progression. We stably transfected pIgR cDNA into two cell lines with low basal pIgR expression: the immortalized normal bronchio-epithelial cell 16-HBE and the lung ADC cell A549 (Figure 3A). For further functional studies, we selected the clones with the strongest stable pIgR expression (16-HBE-pIgR1, A549-pIgR29) and also one clone with moderate stable pIgR expression (A549-pIgR32). All clones transfected with empty vector displayed low basal pIgR expression, therefore we randomly selected control clones (16-HBE-EV1, A549-EV11). Then, we evaluated pIgR effects on cell growth during six days. Inhibition of cell proliferation was observed by WST-1 assay in both 16-HBE-pIgR1 (Figure 3B) and A549-pIgR29 (Figure 3C) ($p<0.001$). Moreover, a dose-dependent effect of pIgR on cell growth was observed when WST-1 assay was performed with A549-EV11 (low basal pIgR expression), A549-pIgR32 (moderate pIgR expression) and A549-pIgR29 (strong pIgR expression) cells (Figure 3D).

pIgR overexpression effect on cell death

To understand the mechanisms by which pIgR decreased cell proliferation, we questioned whether it induces cell cycle arrest and/or increases apoptosis. In our experiments, pIgR transfection did not impact on cell cycle in A549-pIgR29, independently of serum starvation conditions for up to 26h (Figure 4). The apoptotic rate of A549-pIgR29 at baseline was not significantly different than A549-EV11, but there was a tendency for increased apoptosis and necrosis in A549-pIgR29 (Figure 5), which may contribute to the decreased cell proliferation. Then, we questioned whether growth inhibition was related to ER stress induced by pIgR sequestration in ER. Calreticulin and BIP expression, two ER stress markers, was not modified in A549-pIgR29 and 16-HBE-pIgR1 (Figure 6), suggesting the absence of ER stress.

pIgR overexpression is associated with NOTCH3 down-regulation

In search for a mechanism explaining pIgR inhibitory effect on cell growth, we investigated whether the expression of downstream target genes was modified. We used an Affymetrix gene expression array and compared gene expression profiles of A549-pIgR29 and A549-EV11. Among 16830 genes represented on the array, 46 were significantly up-regulated (>2 fold) (Supplementary Table 1A) and 40 significantly down-regulated (>2 fold) (Supplementary Table 1B) in A549-pIgR29. We determined that differentially expressed genes were encoding for membrane and secreted proteins. While membrane proteins represent only 20-30% of total cell proteins [22], 20/46 (43%) of upregulated and 18/40 (45%) of downregulated genes in A549-pIgR29 were encoding for membrane proteins. Moreover, five upregulated and ten downregulated genes were encoding secreted proteins. Overall, 25/46 (54%) of upregulated and 28/40 (70%) of downregulated genes were encoding membrane or secreted proteins. Among upregulated genes, we found pIgR and eight genes involved in induction of differentiation (EGR1, GATA3, IL24, NDN, PLCB4, Rab3B, SPARC, TLE4).

There were also six genes implicated in tumor suppressor properties through cell adhesion and cell-cell/cell-matrix interactions (COL13A1, CYR61, FRMD3, PPAP2B, SPARC, TFPI2).

Among downregulated genes, we found genes involved in metabolic reactions contributing to tumor growth (AQP3, CA12), inhibition of differentiation (NOTCH3), migration and invasion (CNTN1, CSPG2, FN1, VAV3).

We observed that NOTCH3 expression was significantly decreased in A549-pIgR29 and 16-HBE-pIgR1 (Figure 6), validating at the protein level the observations we made by gene expression array. We also tested NOTCH3 expression in lung cancer and normal tissues previously tested for pIgR expression (Figure 2A). We found that NOTCH3 and pIgR were inversely correlated (pIgR upregulation associated with NOTCH3 downregulation and pIgR downregulation associated with NOTCH3 upregulation) in 3/5 lung ADCs and 3/5 SCCs (Supplementary Figure 1).

Discussion

The main objectives of this study were to test whether pIgR expression is downregulated in lung preinvasive lesions, has prognostic implications in patients with lung cancer and plays a role in cellular functions important to cancer development/progression.

To address the first hypothesis, we analyzed pIgR expression by IHC in 10 lung preinvasive lesions. We found that pIgR expression was lost in all tested tissues, suggesting that its downregulation occurs early in lung tumorigenesis. This is a first report of pIgR expression in preinvasive bronchial lesions. Our results are consistent with observations made in colorectal cancer development [16, 18] and suggest a broader role of this protein in tumorigenesis.

To test whether pIgR staining is associated with clinical outcomes, we analyzed pIgR expression by IHC in lung cancer tissues from 175 patients and correlated staining scores with clinical and pathological characteristics. pIgR expression was absent in all undifferentiated NSCLCs, 90% SCCs and 52% ADCs. Overall, pIgR expression was significantly higher in lung cancers of ADC subtype, which is consistent with previous observations [7, 9, 13]. pIgR expression was also significantly higher in younger patients. Decreased pIgR expression with aging was reported in rat liver [23], mouse kidney and gut,[24] but never in human lung. Mechanisms of this age-dependent downregulation are unknown, even though post-transcriptional modifications have been suggested in rat [23]. In our study, pIgR expression was not associated with disease stage or survival. Results were similar whether the analysis was performed with all the 175 patients or limited to the 98 patients with lung ADC. This is in contrast with observations made in other cancers. In gastroesophageal ADCs, tumors without pIgR expression had more frequent lymph node metastases, suggesting that pIgR downregulation identifies a more aggressive phenotype [25]. In colorectal cancers, several

studies proposed pIgR as a prognostic biomarker [14, 16-18, 26]. In three of them, pIgR expression was associated with histological grade [14, 16, 18]. In another one, tumors with low pIgR expression had higher disease stage, shorter recurrence-free survival and increased number of tumor-related deaths [17]. In most of our lung cancer tissues expressing pIgR, staining was heterogeneous, which may explain the absence of association with stage or survival and limit pIgR prognostic value.

Finally, to determine whether pIgR plays a role in functions important to cancer development/progression, we tested the effect of pIgR overexpression in stably transfected A549 on proliferation. We found that pIgR overexpression significantly reduced their proliferation over time and in a dose-dependent manner. This suggests that loss of pIgR expression contributes to lung tumorigenesis and is, to our best knowledge, a first report of an effect of pIgR on cell proliferation.

We pursued our investigations to understand the mechanisms by which pIgR decreases cell proliferation. Our studies showed no evidence for cell cycle arrest or ER stress induced by pIgR overexpression. However, we observed a tendency for increased apoptosis and necrosis in A549-pIgR29, which may contribute to growth inhibition. We also analyzed gene expression profiles of A549-pIgR29 and A549-EV11 by transcriptome analysis. Among differentially expressed genes, we found a high proportion of genes encoding membrane and secreted proteins, with several upregulated genes involved in induction of differentiation and a downregulated (NOTCH3) gene involved in inhibition of differentiation in A549-pIgR29. Moreover, several genes upregulated in A549-pIgR29 were involved in cell adhesion and cell-cell/cell-matrix interactions, which regulate cell differentiation. Based on the observation that pIgR is expressed in a highly polarized way in epithelial cells [1] and that disruption of cell polarity disturbs pIgR trafficking [27], it was previously hypothesized that loss of pIgR expression may have a role in tumor progression through disruption of cell architecture or

physiology [28]. Taken together, our results also suggest that inhibition of proliferation in A549-pIgR29 may be related to increased cellular differentiation. Disruption of normal differentiation is recognized as a hallmark of human cancers [29], and studies in many cell types have shown that proliferation and differentiation are inversely correlated processes, independently from cell cycle [30]. Therefore, pIgR may have an indirect role in the inhibition of cell proliferation by maintaining cellular integrity and differentiation.

To test this hypothesis, we evaluated NOTCH3 protein expression in stably transfected A549 and 16-HBE cells. NOTCH3 is a cell surface receptor overexpressed in several epithelial malignancies, including lung cancers [31], and preventing normal terminal differentiation during oncogenesis [32]. We found that pIgR overexpression in A549 and 16-HBE induced NOTCH3 downregulation, validating the observations made by gene expression analysis. However, all these analyses were performed with cell lines grown under non-polarizing conditions, which make it difficult to support the hypothesis that increased differentiation is the mechanism by which pIgR inhibits cell proliferation. We also tested NOTCH3 expression in primary human lung cancers and, interestingly, we found that NOTCH3 and pIgR were inversely correlated in 6/10 lung cancer tissues. Further studies are warranted to determine the interplay between pIgR and NOTCH3 in cellular differentiation.

In summary, loss of pIgR expression in lung preinvasive lesions suggests that pIgR downregulation is an early event during lung tumorigenesis that is not associated with survival. pIgR overexpression in lung ADC cell line A549 induced inhibition of cell proliferation, upregulation of genes involved in cell differentiation and downregulation of a gene involved in inhibition of differentiation, NOTCH3 [32], suggesting that pIgR may play a role in lung tumorigenesis by maintaining cell differentiation.

Acknowledgements

We thank Dr. Kaetzel for kindly providing us human pIgR cDNA in pcDNA3.1(-). We thank Vanderbilt University DNA Microarray Core Facility for performing Affymetrix gene expression microarray analysis. This work was partially supported by a Discovery grant from Vanderbilt University and the Vanderbilt SPORE in lung cancer CA90949. Dr. Ocak was supported by a grant from Université Catholique de Louvain (Bourse Clinicien-Chercheur), Belgium.

References

1. Kaetzel CS, Mostov K. Immunoglobulin transport and the polymeric immunoglobulin receptor. *In*: Mestecky J, Bienenstock J, Lamm M, Strober W, McGhee J, Mayer L, eds. *Mucosal Immunology*, 3rd edition. Academic Press, San Diego, 2005; pp. 211-250.
2. Norderhaug IN, Johansen FE, Schjerven H, Brandtzaeg P. Regulation of the formation and external transport of secretory immunoglobulins. *Crit Rev Immunol* 1999; 19(5-6): 481-508.
3. Pilette C, Ouadrhiri Y, Godding V, Vaerman JP, Sibille Y. Lung mucosal immunity: immunoglobulin-A revisited. *Eur Respir J* 2001; 18(3): 571-588.
4. Underdown BJ, Schiff JM. Immunoglobulin A: strategic defense initiative at the mucosal surface. *Annu Rev Immunol* 1986; 4: 389-417.
5. Pilette C, Godding V, Kiss R, Delos M, Verbeken E, Decaestecker C, De Paepe K, Vaerman JP, Decramer M, Sibille Y. Reduced epithelial expression of secretory component in small airways correlates with airflow obstruction in chronic obstructive pulmonary disease. *Am J Respir Crit Care Med* 2001; 163(1): 185-194.
6. Delacroix DL, Marchandise FX, Francis C, Sibille Y. Alpha-2-macroglobulin, monomeric and polymeric immunoglobulin A, and immunoglobulin M in bronchoalveolar lavage. *Am Rev Respir Dis* 1985; 132(4): 829-835.
7. Brown RW, Clark GM, Tandon AK, Allred DC. Multiple-marker immunohistochemical phenotypes distinguishing malignant pleural mesothelioma from pulmonary adenocarcinoma. *Hum Pathol* 1993; 24(4): 347-354.
8. Espinoza CG, Balis JU, Saba SR, Paciga JE, Shelley SA. Ultrastructural and immunohistochemical studies of bronchiolo-alveolar carcinoma. *Cancer* 1984; 54(10): 2182-2189.

9. Harris JP, South MA. Secretory component: a glandular epithelial cell marker. *Am J Pathol* 1981; 105(1): 47-53.
10. Kawai T, Torikata C, Suzuki M. Immunohistochemical study of pulmonary adenocarcinoma. *Am J Clin Pathol* 1988; 89(4): 455-462.
11. Kondi-Paphitis A, Addis BJ. Secretory component in pulmonary adenocarcinoma and mesothelioma. *Histopathology* 1986; 10(12): 1279-1287.
12. Loosli H, Hurlimann J. Immunohistological study of malignant diffuse mesotheliomas of the pleura. *Histopathology* 1984; 8(5): 793-803.
13. Popper H, Wirsberger G, Hoefler H, Denk H. Immunohistochemical and histochemical markers of primary lung cancer, lung metastases, and pleural mesotheliomas. *Cancer Detect Prev* 1987; 10(3-4): 167-174.
14. Arends JW, Wiggers T, Thijs CT, Verstijnen C, Swaen GJ, Bosman FT. The value of secretory component (SC) immunoreactivity in diagnosis and prognosis of colorectal carcinomas. *Am J Clin Pathol* 1984; 82(3): 267-274.
15. Chang Y, Lee TC, Li JC, Lai TL, Chua HH, Chen CL, Doong SL, Chou CK, Sheen TS, Tsai CH. Differential expression of osteoblast-specific factor 2 and polymeric immunoglobulin receptor genes in nasopharyngeal carcinoma. *Head Neck* 2005; 27(10): 873-882.
16. Isaacson P. Immunoperoxidase study of the secretory immunoglobulin system in colonic neoplasia. *J Clin Pathol* 1982; 35(1): 14-25.
17. Koretz K, Schlag P, Quentmeier A, Moller P. Evaluation of the secretory component as a prognostic variable in colorectal carcinoma. *Int J Cancer* 1994; 57(3): 365-370.
18. Krajci P, Meling GI, Andersen SN, Hofstad B, Vatn MH, Rognum TO, Brandtzaeg P. Secretory component mRNA and protein expression in colorectal adenomas and carcinomas. *Br J Cancer* 1996; 73(12): 1503-1510.

19. Khattar NH, Lele SM, Kaetzel CS. Down-regulation of the polymeric immunoglobulin receptor in non-small cell lung carcinoma: correlation with dysregulated expression of the transcription factors USF and AP2. *J Biomed Sci* 2005; 12(1): 65-77.
20. Qian J, Zou Y, Rahman JS, Lu B, Massion PP. Synergy between phosphatidylinositol 3-kinase/Akt pathway and Bcl-xL in the control of apoptosis in adenocarcinoma cells of the lung. *Mol Cancer Ther* 2009; 8(1): 101-109.
21. Tamer CM, Lamm ME, Robinson JK, Piskurich JF, Kaetzel CS. Comparative studies of transcytosis and assembly of secretory IgA in Madin-Darby canine kidney cells expressing human polymeric Ig receptor. *J Immunol* 1995; 155(2): 707-714.
22. Stevens TJ, Arkin IT. Do more complex organisms have a greater proportion of membrane proteins in their genomes? *Proteins* 2000; 39(4): 417-420.
23. van Bezooijen RL, Wang RK, Lechner MC, Schmucker DL. Aging effects on hepatic NADPH cytochrome P450 reductase, CYP2B1&2, and polymeric immunoglobulin receptor mRNAs in male Fischer 344 rats. *Exp Gerontol* 1994; 29(2): 187-195.
24. Yanagihara T, Kumagai Y, Norose Y, Moro I, Nanno M, Murakami M, Takahashi H. Age-dependent decrease of polymeric Ig receptor expression and IgA elevation in ddY mice: a possible cause of IgA nephropathy. *Lab Invest* 2004; 84(1): 63-70.
25. Gologan A, Acquafondata M, Dhir R, Sepulveda AR. Polymeric immunoglobulin receptor-negative tumors represent a more aggressive type of adenocarcinomas of distal esophagus and gastroesophageal junction. *Arch Pathol Lab Med* 2008; 132(8): 1295-1301.
26. Rognum T, Elgjo K, Brandtzaeg P, Orjasaeter H, Bergan A. Plasma carcinoembryonic antigen concentrations and immunohistochemical patterns of epithelial marker antigens in patients with large bowel carcinoma. *J Clin Pathol* 1982; 35(9): 922-933.

27. Chintalacharuvu KR, Piskurich JF, Lamm ME, Kaetzel CS. Cell polarity regulates the release of secretory component, the epithelial receptor for polymeric immunoglobulins, from the surface of HT-29 colon carcinoma cells. *J Cell Physiol* 1991; 148(1): 35-47.
28. Traicoff JL, De Marchis L, Ginsburg BL, Zamora RE, Khattar NH, Blanch VJ, Plummer S, Bargo SA, Templeton DJ, Casey G, Kaetzel CS. Characterization of the human polymeric immunoglobulin receptor (PIGR) 3'UTR and differential expression of PIGR mRNA during colon tumorigenesis. *J Biomed Sci* 2003; 10(6 Pt 2): 792-804.
29. Hanahan D, Weinberg RA. The hallmarks of cancer. *Cell* 2000; 100(1): 57-70.
30. Brown G, Hughes PJ, Michell RH. Cell differentiation and proliferation--simultaneous but independent? *Exp Cell Res* 2003; 291(2): 282-288.
31. Dang TP, Gazdar AF, Virmani AK, Sepetavec T, Hande KR, Minna JD, Roberts JR, Carbone DP. Chromosome 19 translocation, overexpression of Notch3, and human lung cancer. *J Natl Cancer Inst* 2000; 92(16): 1355-1357.
32. Dang TP, Eichenberger S, Gonzalez A, Olson S, Carbone DP. Constitutive activation of Notch3 inhibits terminal epithelial differentiation in lungs of transgenic mice. *Oncogene* 2003; 22(13): 1988-1997.

Conflicts of interest

The authors declare no conflict of interest.

Tables

Table 1. pIgR expression in normal, preinvasive and lung cancer tissues.

Cytology/histology		pIgR positive tissues, n (%)	Average pIgR staining scores, /300 (SD)	
			All tissues	pIgR positive tissues
Normal	Mucous cells, n=11	10 (91)	227 (85)	250 (41)
	Serous cells, n=11	10 (91)	227 (85)	250 (41)
	Ciliated cells, n=11	10 (91)	45 (25)	50 (20)
	Alveolar cells, n=11	0	0	0
Preinvasive	Low grade, n=4	0	0	0
	High grade, n=6	0	0	0
Cancer	ADC, n=98	47 (48)	26 (43)	55 (47)
	SCC, n=67	7 (10)	7 (27)	62 (62)
	Undifferentiated NSCLC, n=10	0	0	0

Abbreviations: SD = standard deviation; ADC = adenocarcinoma; SCC = squamous cell carcinoma; NSCLC = non small-cell lung carcinoma.

Table 2. Patient characteristics and statistical significance of the association with pIgR staining intensity.

	n (%)	IQR	95% CI	p values
Gender				0.192
Male	113 (65)			
Female	62 (35)			
Race				0.066
Caucasian	162 (93)			
African American	13 (7)			
Age at diagnosis				
Median, years		66 (58-72)		0.041
≤ 60 years	61 (35)			0.031
> 60 years	114 (65)			
Smoking status				
Current smoker	59 (34)			0.61
Ex-smoker	104 (60)			
Never smoker	10 (6)			
Median pack year smoking history		50 (30-80)		0.086
Median predicted DLCO, %		76 (57-96)		0.976
Median predicted FEV1, %		68 (54-85)		0.703
Lung cancer histology				<.0001
ADC	98 (56)			
SCC	67 (38)			
Undifferentiated NSCLC	10 (6)			
Path stage				0.151
I	102 (58)			
II	19 (11)			
III	35 (20)			
IV	19 (11)			
Path T				0.460
T1	68 (40)			
T2	63 (37)			
T3	18 (11)			
T4	22 (13)			
Path N				0.095
N0	132 (78)			
N1	12 (7)			
N2	26 (15)			
Path M				0.332
M0	156 (89)			
M1	19 (11)			
Recurrence- or progression-free survival				
Median, years			4 (2.6-6.8)	0.411
Recurrence- and progression-free at 3 years	109 (63)			0.580
Overall survival				
Median, years			3 (2.4-4.5)	0.484
Alive at 3 years	90 (51)			0.978
pIgR average staining score				
Score = 0	121 (69)			
Score ≥ 20	41 (23)			
Score ≥ 50	27 (15)			
Score ≥ 100	12 (7)			

Abbreviations: IQR = interquartile range; CI = confidence interval; ADC = adenocarcinoma;
SCC = squamous cell carcinoma; NSCLC = non small-cell lung carcinoma.

Figure legends

Figure 1. pIgR expression in normal bronchial epithelium, in preinvasive lung lesions and in lung cancers evaluated by immunohistochemistry (IHC). **A.** IHC on normal lung tissues revealed a strong staining for pIgR in mucous and serous cells in surface and glandular epithelium, a weak staining in ciliated cells, and an expected absence of staining in alveolar cells. **B-C.** There was no pIgR expression in preinvasive lung lesions (B: squamous metaplasia, C: severe dysplasia). **D-E-F.** pIgR expression was also absent in 90% of squamous cell carcinomas (D: SCC with absence of pIgR staining), while in 52% of adenocarcinomas (E: ADC with absence of pIgR staining, F: ADC with strong pIgR staining). *Pictures magnification: x400.* **G-H.** Kaplan-Meier analysis of overall survival (G) and recurrence or progression-free (R/P-free) survival (H) didn't show survival difference between lung cancer patients with and those without pIgR expression.

Figure 1

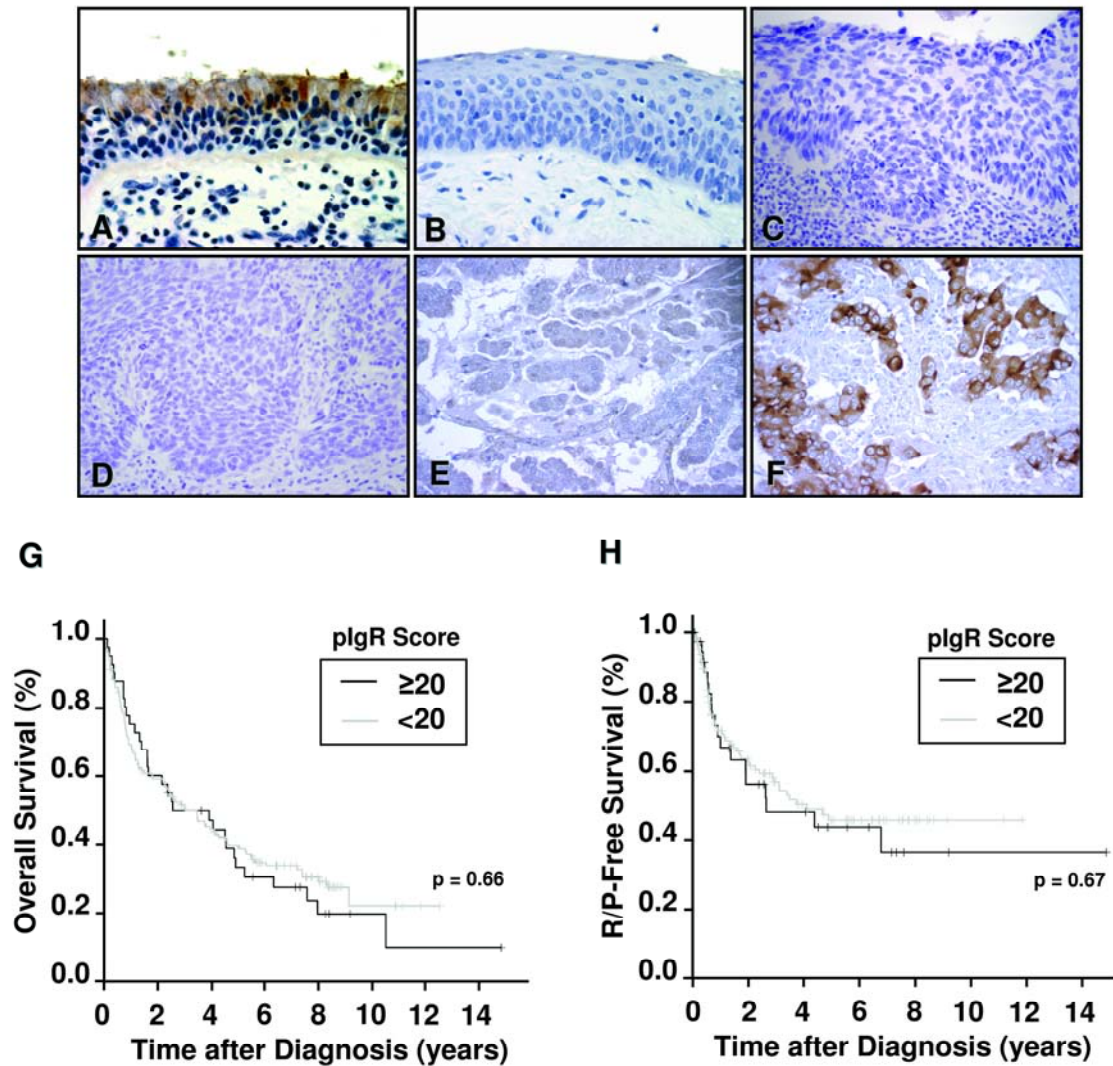


Figure 2. pIgR expression in lung tissues and cell lines evaluated by Western blot. Whole tissue or cell lysates were resolved with SDS-PAGE and blots were incubated with anti-pIgR antibody. pIgR expression levels were normalized to actin. **A.** Lung cancer tissues (T) were compared to normal lung tissues (N) from same patients. The results show downregulation of pIgR expression in 6/6 squamous cell carcinomas (SCC) and in 5/11 adenocarcinomas (ADC), while pIgR was overexpressed in 4/11 ADCs and no expression difference was noted in 2/11 ADCs. **B.** pIgR expression was low in 2/2 transformed normal bronchial epithelial cell

lines, 1/1 undifferentiated non-small cell lung cancer (NSCLC) cell line, 1/1 large cell carcinoma (LCC) cell line, 5/5 squamous cell carcinoma (SCC) cell lines and 7/9 adenocarcinoma (ADC) cell lines. pIgR expression was moderate to strong in 2/9 ADC cell lines.

Figure 2

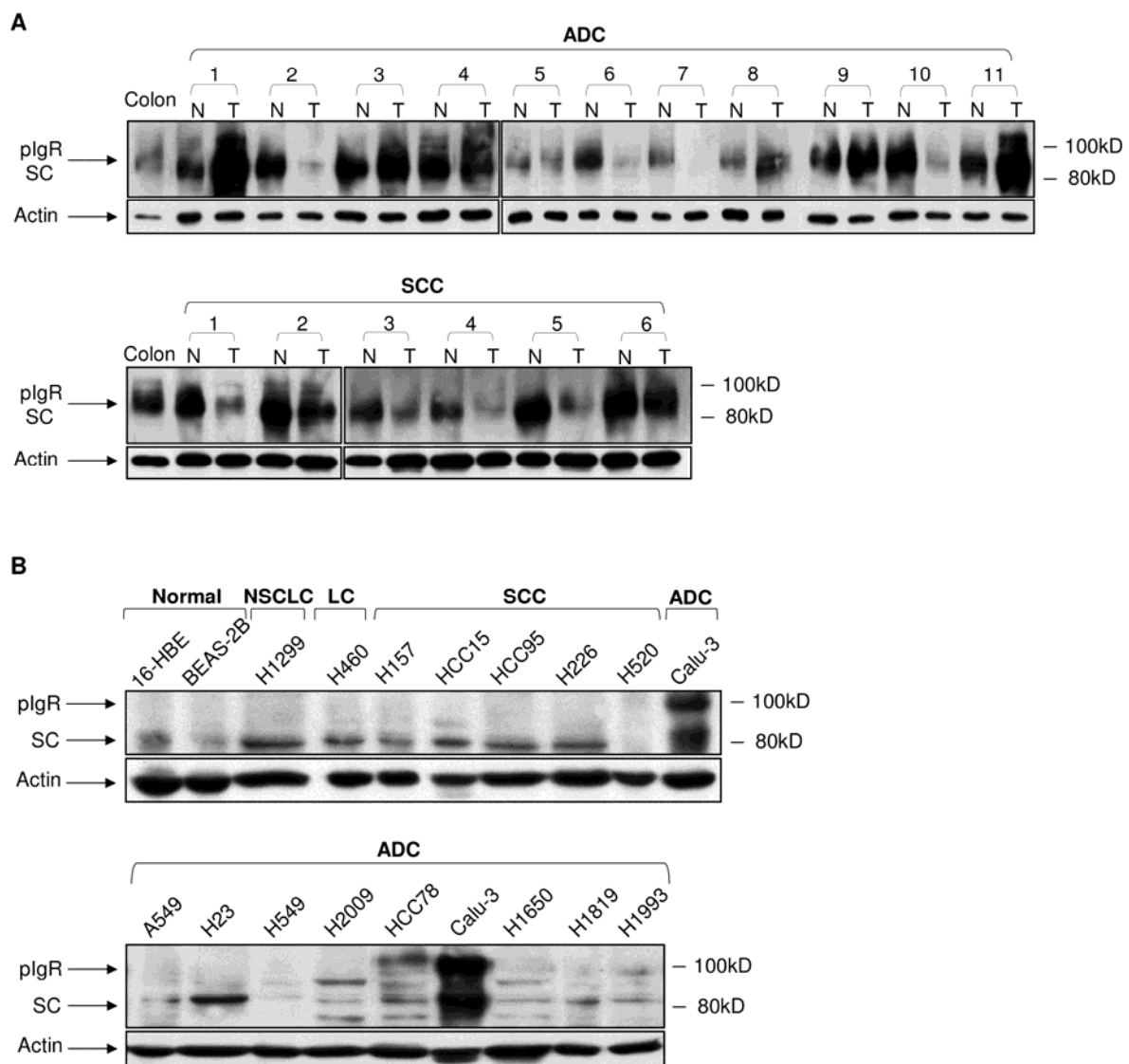


Figure 3. Effects of pIgR overexpression on 16-HBE and A549 proliferation. A. Whole cell lysates were resolved with SDS-PAGE and blots were incubated with anti-pIgR antibody. pIgR expression levels were normalized to actin. Higher expression of pIgR was confirmed

by WB in immortalized normal bronchial epithelial cell line 16-HBE and lung adenocarcinoma cell line A549 stably transfected with pIgR pcDNA3.1(-) (16-HBE-pIgR1, A549-pIgR29 and A549-pIgR32) as compared to empty vector pcDNA3.1(-) (16-HBE-EV1 and A549-EV11). pIgR expression was higher in A549-pIgR29 (clone with the strongest pIgR expression) than in A549-pIgR32 (clone with moderate pIgR expression). **B.** Inhibition of cell growth was observed by WST-1 assay in 16-HBE-pIgR1 grown for six days as compared to 16-HBE-EV1. Optical density (OD) in Y axes reflects the proportion of metabolically active cells. **C.** Inhibition of cell growth was observed by WST-1 assay in A549-pIgR29 grown for six days as compared to A549-EV11. **D.** Dose-dependent effect on cell growth inhibition in A549 cells. Inhibition of cell growth was less pronounced in A549-pIgR32 (clone with moderate expression of pIgR) than in A549-pIgR29 (clone with higher expression of pIgR). *Error bars: +/-1 standard deviation (n=5 in WST-1 and n=3 in cell number count). All the graphs represent one of three independent experiments with similar results.*

Figure 3

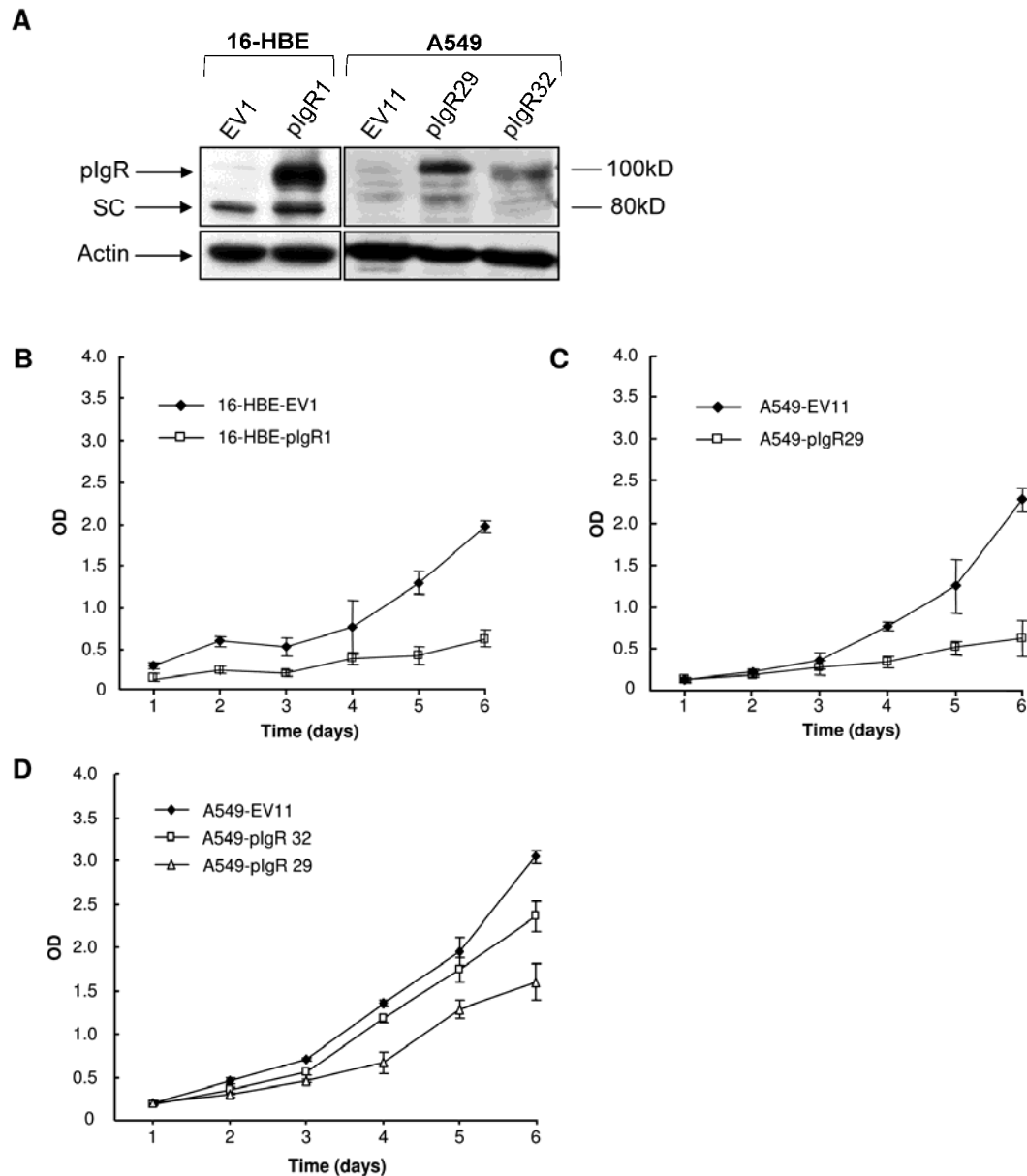


Figure 4. Effects of pIgR overexpression on A549 cell cycle evaluated by flow cytometry with nuclear propidium iodide staining. A. Flow cytometry profiles of cell cycle distribution in stably transfected A549-EV11 and A549-pIgR29, representative of three experiments with similar results. **B.** This figure represents the average of three independent experiments and shows that the percentage of cells in pre-G1 (apoptosis), G1, G2 and S

phases was not statistically different in A549-EV11 and A549-pIgR29. *Error bars: ± 1 standard deviation ($n=3$).*

Figure 4

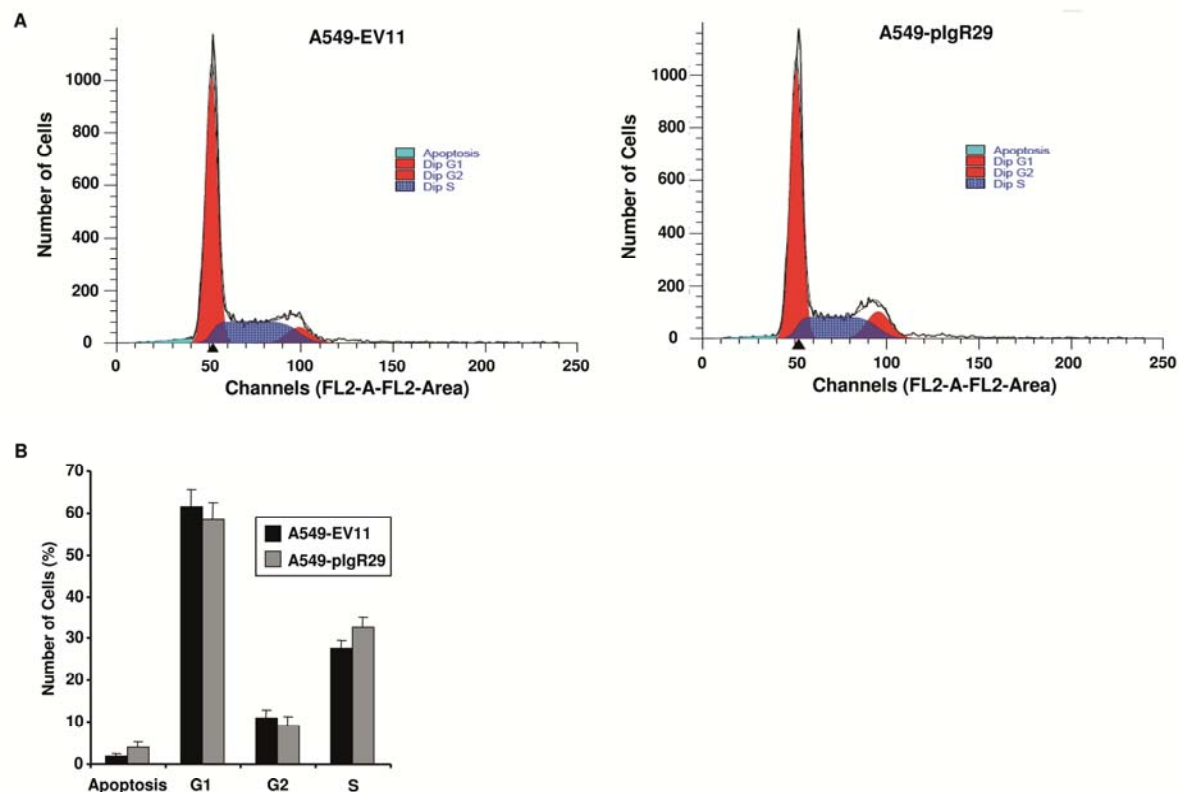


Figure 5. Effects of pIgR overexpression on A549 apoptosis evaluated by Annexin V apoptosis assay. Stably transfected cells were stained with Annexin V and propidium iodide (PI), and the staining was quantified by FACS analysis. **A.** Quadrant dot blot analysis of A549-EV11 and A549-pIgR29 cells stained for apoptosis using an annexin V detection of phosphatidyl serine expression along the X-axis, counterstained with PI to detect late apoptotic or necrotic cells along the Y-axis. In the lower left quadrant are found viable non-apoptotic cells, apoptotic cells binding annexin V in the lower right. Cells in the upper right are late apoptotic cells binding annexin V and taking up PI, and in the upper left are necrotic cells taking up PI but not binding annexin V. These figures are representative of three independent experiments. **B.** This figure represents the average of three independent

experiments and shows that the spontaneous level of early apoptosis, late apoptosis and necrosis had a tendency to be higher in cells overexpressing pIgR (A549-pIgR29), but the difference was not statistically significant. *Error bars: +/-1 standard deviation (n=3).*

Figure 5

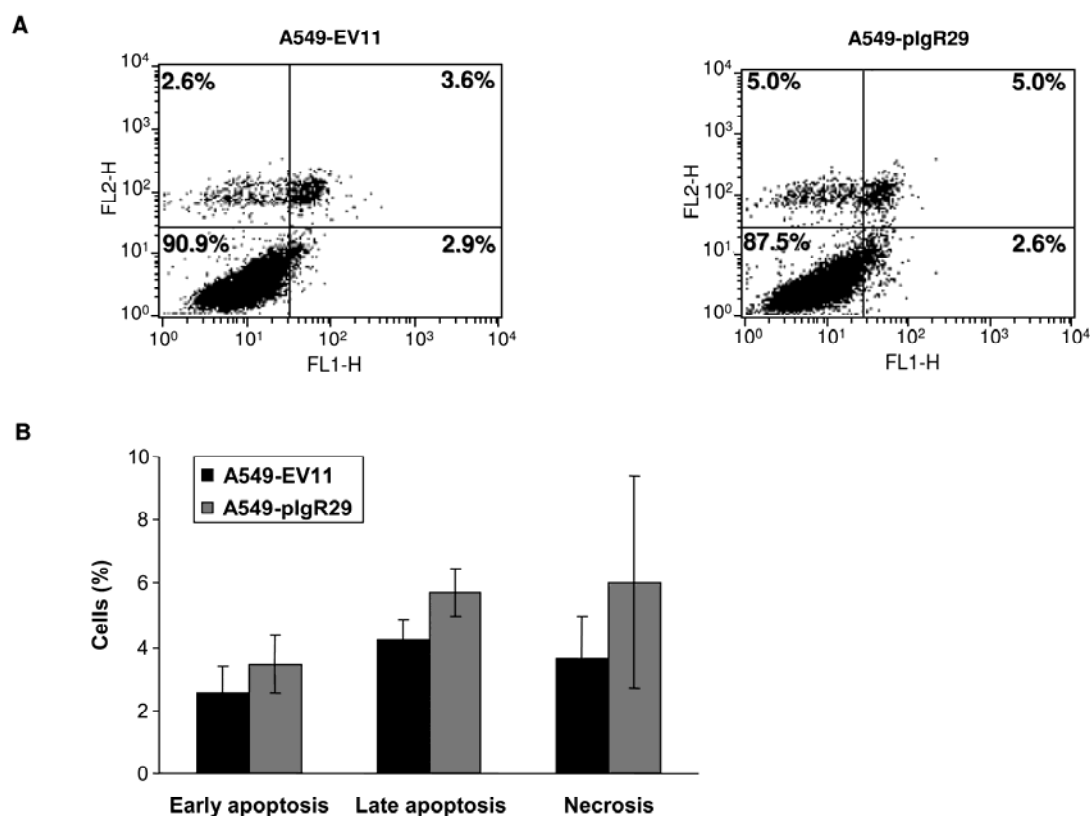
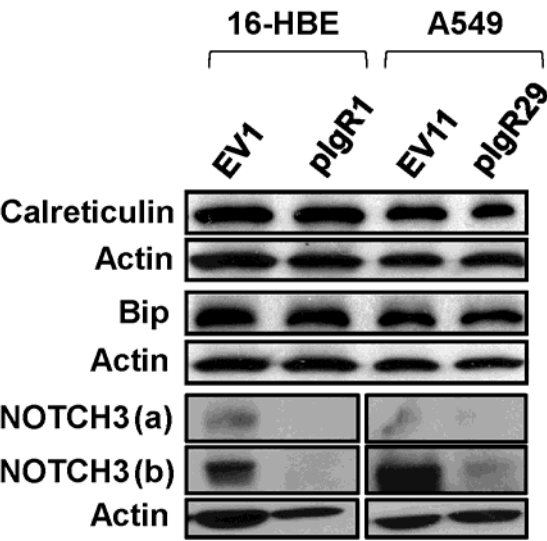


Figure 6. Effects of pIgR stable overexpression on endoplasmic reticulum stress markers evaluated by WB. Whole cell lysates were resolved with SDS-PAGE and blots were incubated with anti-pIgR, calreticulin, BIP and NOTCH3 antibodies. Expression levels of these proteins were normalized to actin. pIgR overexpression didn't affect the expression of ER stress markers calreticulin and BIP, but decreased NOTCH3 expression. *NOTCH3 (a): full-length NOTCH3; NOTCH3 (b): NOTCH-derived peptide containing the intracellular domain of NOTCH3.*

Figure 6



Supplementary data

Supplementary table 1A. Up-regulated genes expression (>2 folds) in A549-pIgR29 cells as compared to A549-EV11 by Affymetrix gene expression microarray analysis.

Supplementary table 1B. Down-regulated genes expression (>2 folds) in A549-pIgR29 cells as compared to A549-EV11 by Affymetrix gene expression microarray analysis.

Supplementary Figure 1. Correlation between pIgR and NOTCH3 expression in lung cancer tissues. Whole tissue lysates were resolved with SDS-PAGE and blots were incubated with anti-pIgR and NOTCH3 antibodies. Expression levels of these proteins were normalized to actin. NOTCH3 and pIgR levels were inversely correlated (upregulation of pIgR associated with downregulation of NOTCH3 and downregulation of pIgR associated with upregulation of NOTCH3) in 3/5 lung adenocarcinomas (ADCs) and 3/5 squamous cell carcinomas (SCCs). *NOTCH3 (a): full-length NOTCH3; NOTCH3 (b): NOTCH-derived peptide containing the intracellular domain of NOTCH3.*